99-89

ELSEVIER

Composites Science and Technology 60 (2000) 2713–2724

COMPOSITES SCIENCE AND TECHNOLOGY

www.elsevier.com/locate/compscitech

Optical and acoustic damage detection in laminated CFRP composite materials

L. Rippert [a,*], M. Wevers [a], S. Van Huffel [b]

[a] *Katholieke Universiteit Leuven, Faculty of Applied Sciences, Department of Metallurgy and Materials Engineering (MTM), W. De Croylaan 2, B-3001 Leuven, Heverlee, Belgium*

[b] *Katholieke Universiteit Leuven, Faculty of Applied Sciences, Department of Electrical Engineering (ESAT-SISTA/COSIC), K. Mercierlaan 94, B-3001 Leuven Heverlee, Belgium*

Received 15 October 1999; received in revised form 22 May 2000; accepted 6 June 2000

Abstract

Composite materials would gain substantial added value if it were possible to equip them with a system that could continuously monitor their damage state. In this approach, fibre-optic sensors could offer an alternative to the robust piezoelectric transducers used for acoustic emission (AE) monitoring. An intensity-modulated sensor based on the microbending concept was built and used to detect damage in laminated CFRP composite materials. Pencil lead break tests and tensile tests have been performed. The short-time Fourier Transform (STFT) has been computed and noise-reduction algorithms (adaptive filtering and spectral subtraction filtering) have also been used. The specimen final fracture can clearly be seen but transient signals were also detected before this final event. They can be correlated with the acoustic emission signals, analysed by a classical AE parameter study and with a modal acoustic emission (MAE) system. It is thus shown that the optical signal contains information on the elastic energy released whenever damage is being introduced in the host composite. Hints are that time-frequency analysis could be used to characterise this damage in a way similar to what is done for MAE. © 2000 Elsevier Science Ltd. All rights reserved.

Keywords: A. Polymer-matrix composites; B. Fracture; D. Acoustic emission; Fibre optic sensors

1. Introduction

The emergence of optical-fibre communication technologies in the 1970s has enabled the development of embedded optical sensors for process condition monitoring and for smart material/structure applications. Meanwhile, thanks to the evolution in computer technology, powerful data analysis tools have appeared. With optical fibres embedded in composite materials and advanced data processing of the optical fibre signals, a non-destructive testing (NDT) system can be integrated into this complex material, component or structure similar to the neural system in a human body. In this approach fibre-optic sensors [1] will offer an alternative to the robust piezoelectric transducers used for acoustic emission (AE) monitoring.

Indeed fibre-optic sensors have several advantages compared to the electronically based sensors like piezoceramics such as light-weight, all-passive configurations, low power utilisation, immunity to electromagnetic interference, high sensibility and bandwidth, compatibility with optical data transmission and processing, long lifetimes and low cost (provided silicon fibres are used). The difficulties to overcome to obtain reliable data are the complex signal processing and the embedding procedure of the optical fibre (influence on the host material properties and connections with the outside world) [2,3].

Two kinds of optical-fibre sensors can be used: intensity-modulated sensors and phase-modulated sensors (interferometers).

Different configurations for phase-modulated sensors can be set namely the Michelson interferometer, the Mach-Zenhder interferometer and the Fabry-Perot interferometer. They have been successfully used for acoustic wave detection [4–6] and damage detection in various materials [7] and in particular composite materials [4,8,9]. Phase-modulated sensors are usually very sensitive but also very complex and fragile.

* Corresponding author. Fax: +32-016-32-19-90.
E-mail address: laurent.rippert@mtm.kuleuven.ac.be (L. Rippert).

0266-3538/00/$ - see front matter © 2000 Elsevier Science Ltd. All rights reserved.
PII: S0266-3538(00)00135-4

Intensity-modulated sensors detect variations in the intensity of the transmitted light caused by a perturbing environment. The main causes for intensity modulation are transmission, reflection and microbending. The major limitation for these sensors is that any intensity fluctuations in the output not associated with the measurand produce erroneous results. Various schemes can be used to self-reference sensors and so correct this problem [10]. Several intensity-modulated sensors have been successfully used to measure damage but they usually rely on the optical fibre fracture [11,12]. The first intensity-modulated sensors developed, used the microbending concept to detect pressure, acceleration, displacement, temperature and strain [10,13–15]. Intensity-modulated optical fibre sensors require only a simple and robust sensing system.

In this study, it will be shown that the optical signal, collected from an intensity-modulated sensor based on the microbending concept, contains information not only on the strains in the composite due to remote loading but also on the elastic energy and hence strain released whenever suddenly damage is being introduced in the host material. Advanced signal processing techniques based on time-frequency analysis are applied to obtain these results which are compared with those obtained from an acoustic emission monitoring system.

2. Principle of operation

In the microbending concept (see Fig. 1), the physical property to be measured is converted into a displacement which bends the fibre at certain locations. If an optical fibre is bent, small amounts of light are lost through the cladding because the condition of total reflection is violated. The amount of intensity loss depends on the amount of bending and thus on the amount of displacement [2]. The stress field in a damaged layer is not the same as in an undamaged layer. This may cause the optical fibre to bend in the material. So the initiation of damage should correspond to a decrease in the intensity of the transmitted light as it was shown by M. Surgeon [16]. This concept can be explored further. Damage can also be characterised by mechanical waves propagating in the material. When a wave hits an optical fibre, the stress bends it locally and so some light might also be lost (coupling between propagating and radiation modes). A high sampling rate (SR) can be used to detect transient signals which could be stress waves released by matrix cracking, delamination or fibre fracture phenomena. This requires signal analysis tools such as filtering, time analysis and time-frequency analysis (STFT). This paper will focus mainly on the signal analysis tools.

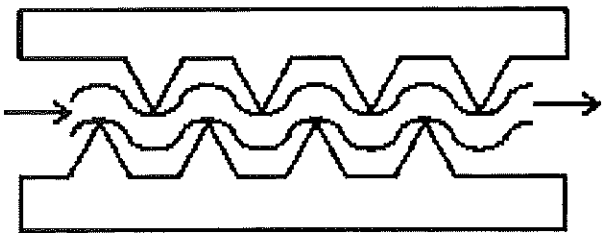


Fig. 1. The microbending concept.

3. Experimental

An HeNe laser source is used with a multimode optical fibre embedded in a carbon fibre reinforced composite material. The output signal light intensity is collected by a photo-diode, and is sent to a computer via an oscilloscope as seen in Fig. 2. The signal treatment was done using MATLAB® software. The short time Fourier transform (STFT) is computed, time and time-frequency analyses are performed.

A multimode optical fibre (FIP100110125 from Polymicro Technology Inc.) was connected to a 20 mW laser source (LGK 7654-7 from LASOS) via an optical coupler (HUC 13-633-M-2.6 GR-2 from OZ OPTICS Ltd.). The optical fibre diameters were 100 μm for the core, 110 μm for the cladding and 125 μm for the polyimide coating.

Laminates were produced from a Vicotex 6376/35/137/T400 C/epoxy prepreg. The prepreg was cut and stacked into a $[0_2°, 90_4°]_s$ lay-up. The optical fibre was embedded in the 90° direction in the middle plane of the specimen. A polymeric bore tube was put around the optical fibre at its exit point from the composite specimen. It shrank around the fibre during the cure and so protected this weak point [17]. The samples were cut from the plates at a length of 150 mm, a width of 25 mm and a thickness of 1.2 mm.

The optical fibre characteristics have been chosen to maximise the light intensity and the strain/stress transfer from the composite material to the optical fibre. The small diameter difference between the core and the cladding increased the loss of light due to bending. The influence of optical fibre embedment on the host material has received a lot of attention in the past for tension, compression, bending and fatigue loading [17–21]. The compressive strength is the most reduced material characteristic especially if the optical fibre is embedded in perpendicular direction to the loading. It is well known that embedding the optical fibre in a parallel direction with the reinforcing fibres can reduce these effects especially if an optical fibre with a small outer diameter (less than 150 μm) is used.

The optical signal was collected in a photodiode (D-series pin photodiode from UDT Sensor Inc.), further amplified (UDT-1200A Medium Speed Amplifier from UDT Sensor Inc.) and sent to a digital oscilloscope (LeCroy 9310AM Dual 400 MHz Oscilloscope 100 Ms/s

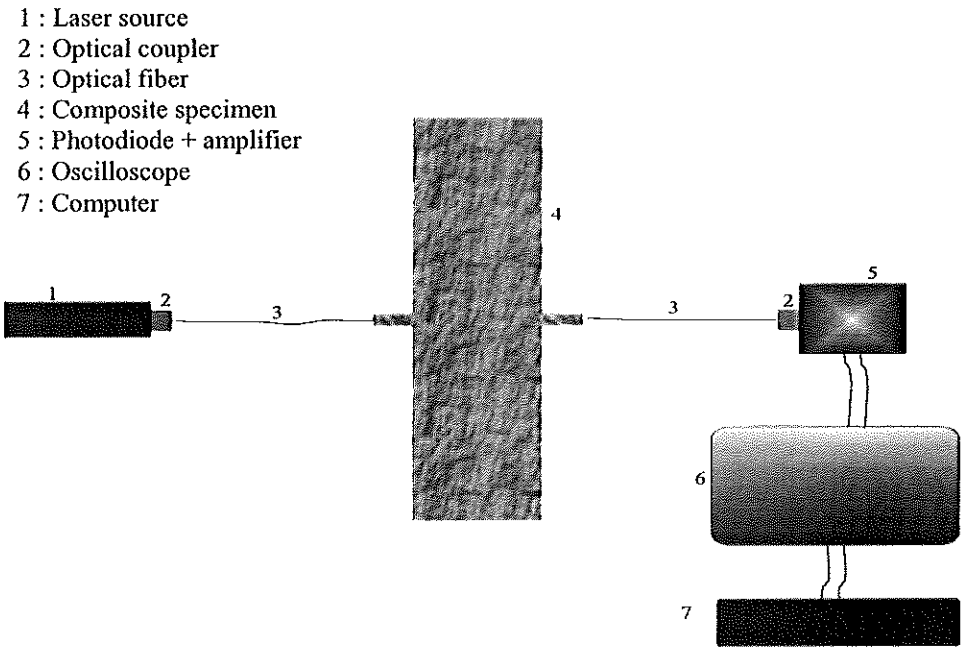


Fig. 2. The optical sensing system.

200 Kpts/Ch.) with an 8 bits A/D converter. The signal was then stored in a computer via a GPIB protocol.

The optical signal post-processing was done on a SUN workstation using MATLAB® software, in particular the signal processing toolbox. A program was written to filter the signal, to compute its STFT and to visualise the changes in its power spectrum over time [22]. Additional tools were developed to extract damage related information from this time-frequency analysis.

Tensile tests have been performed on the 4505 Instron testing machine with a 100 kN loadcell. To be certain that the specimens did not slip in the grips, aluminium end tabs were bonded to the specimens using a two components Araldite 2011 epoxy glue. The Instron machine was operated at 0.5 mm/min displacement rate. A homemade Labview program drove the tensile machine and the oscilloscope. For high SR, the optical system needed to be stopped regularly to give the oscilloscope enough time to empty its memory buffer. During this time the loading was also stopped, so the load was not applied continuously (see Fig. 3) but stepwise.

Two acoustic emission (AE) systems were also used to detect the damage development in the composite material.

The first system, AMS3 Vallen Systeme, used two piezoelectric sensors (DECI 375M) with a resonance frequency of 375 kHz. Events vs. time curves could be drawn (as seen in Fig. 4) and classical AE parameters were computed (amplitude, energy, duration and ring-down count) for each of the located events.

It is difficult to recognise real damage events from noise and to characterise the kind of damage from the classical AE parameters. The first results found in the literature were quite contradictory. Now, most agree that AE events can be sorted according to one or more

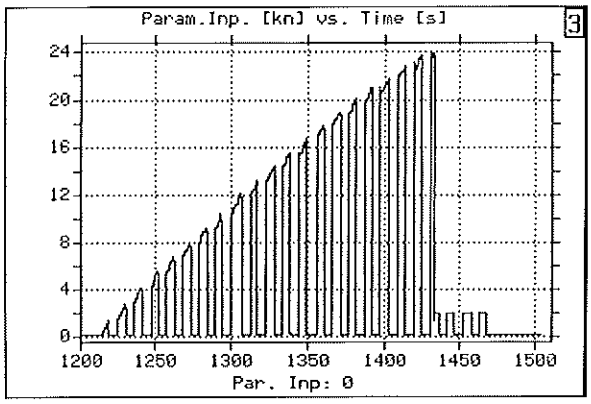


Fig. 3. The load versus time.

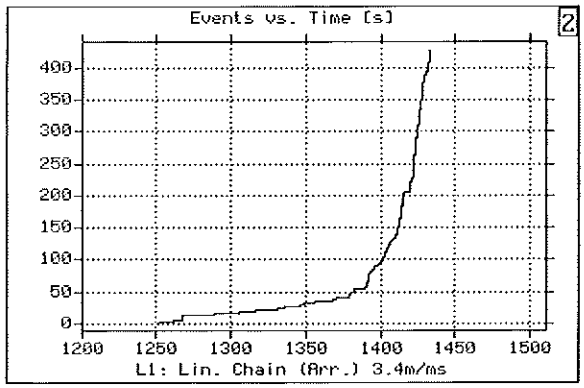


Fig. 4. The AE events versus time.

AE signal parameters and thus identify different damage modes [23].

The second system, Wave Explorer from Digital Wave Corp., needs broadband sensors (Digital Wave B1025) with a nearly flat frequency response in the 50–3000 kHz frequency range. It uses the plate wave theory as a theoretical background and the waves are analysed according to their mechanical nature, namely extensional and flexural waves. It is called a modal acoustic emission (MAE) system [24, 25].

MAE allows a more convenient way to identify damage modes by looking at the frequency content of the acoustic waves produced by the damage. The presence (or absence) of extensional and flexural modes is the key to the damage mode characterisation. It has been proven to work in an efficient way for matrix cracking and fibre fracture [26]. It also allows a clear recognition of noise grip and EMI.

4. Results and discussion

Ten specimens were tested. For each tensile test, the moment of the final specimen fracture was first searched for in the optical fibre signal recording. Then, the rest of the test was studied to try to correlate the optical signal

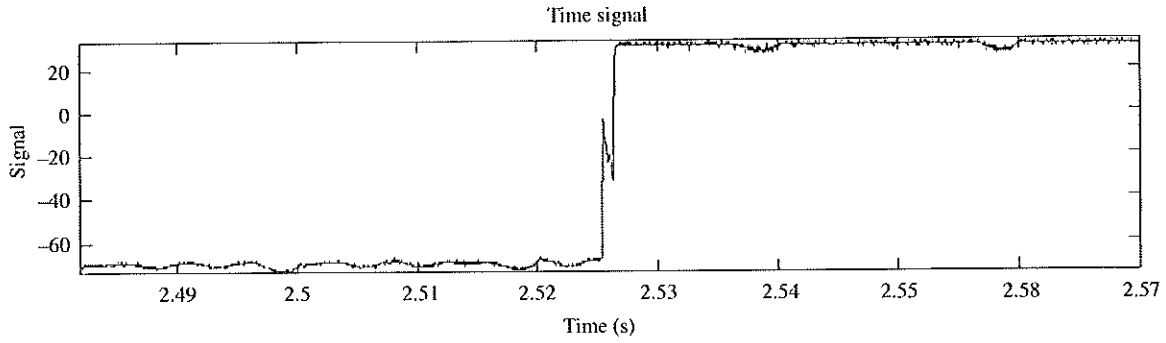


Fig. 5. The optical signal versus time; the sampling rate (SR) is 50 kHz.

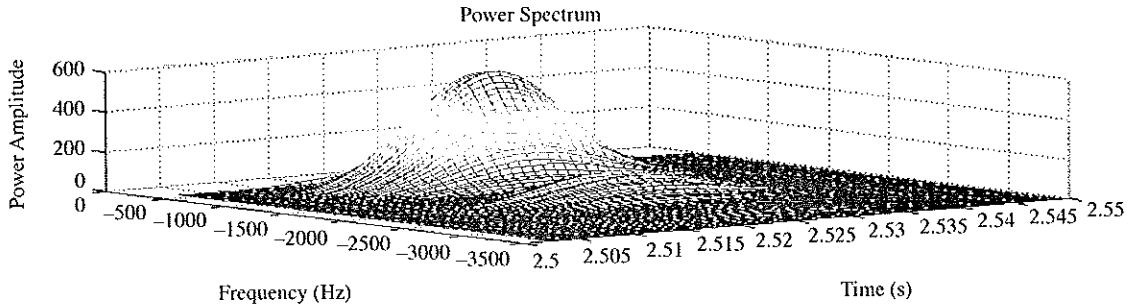


Fig. 6. A 3D plot of the spectrogram of the optical signal ($SR = 50$ kHz, $N = 2048$ samples, $I = 1$ ms, so $\Delta f = 24.4$ Hz and $\Delta T = 41$ ms).

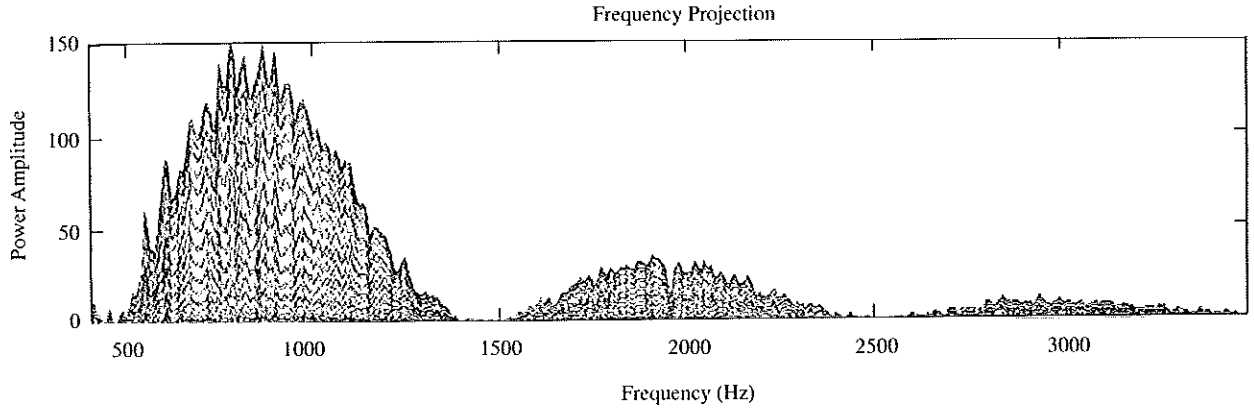


Fig. 7. The frequency projection of the spectrogram ($SR = 50$ kHz, $N = 8192$ samples, $I = 20$ ms and $\Delta f = 6$ Hz).

with the AE signal. To do this, several noise reduction techniques were applied and pencil lead break tests were also performed for a calibration purpose.

4.1. The final specimen fracture

In five tests the optical fibre was not broken during the specimen fracture, so the whole final fracture could be recorded optically as can be seen in Fig. 5.

From this figure (time domain), it can be deduced that for this specimen the final fracture happened in two steps. The two spikes were found to be 1.08 ms apart. It was localised in time (at $T_0 = 2.525$ s) with a precision of 20 μs. A higher sampling rate would give a better time precision.

Due to the AE system time resolution, the final specimen fracture was seen by AE as a unique event whose characteristics were notably higher than the other events recorded, for instance:

Amplitude:	93.9 dB (saturation)
Duration:	4.7 ms
Energy:	5.2 10^6 eV
Ringdown Count:	1168

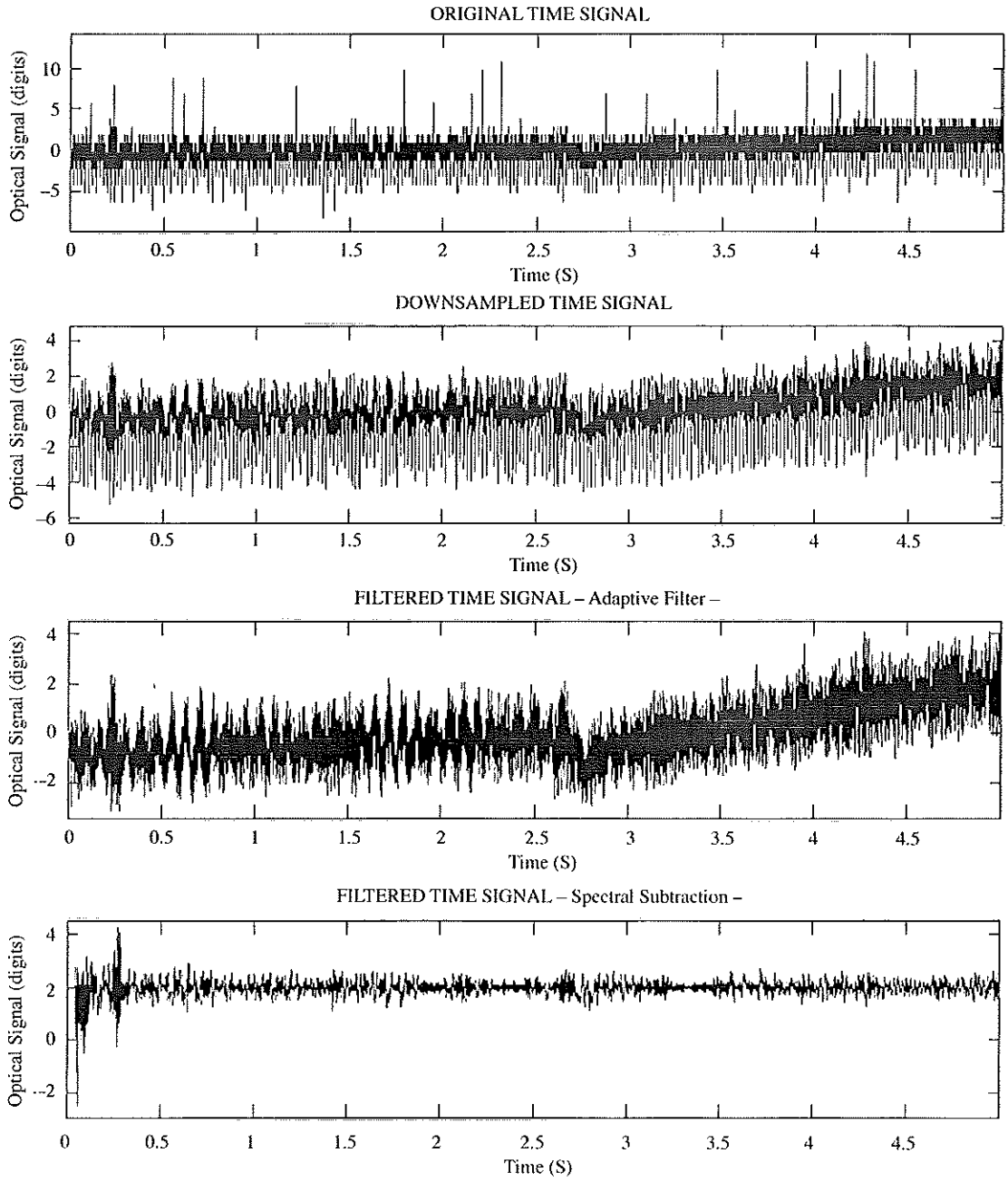


Fig. 8. The optical signal (time domain) from top to bottom: the original optical signal ($SR = 50$ kHz) is downsampled to 10 kHz, then filtered with an adaptive filter (step parameter $\mu = 0.01$) and finally filtered again using spectral subtraction.

4.1.1. Signal analysis tools (time-frequency analysis)

In this study the signal was non-stationary (and transient signals were also expected), so its frequency content, visualised by the Fourier transform, varied in time. The STFT can be used to visualise the frequency content of a signal over time.

The optical signal was multiplied with a Hanning window of a certain length of time ΔT and Fourier transformed. The window was then moved over a time interval I and the same procedure was repeated. The squared amplitudes of all these Fourier transforms were displayed along the time axis corresponding to the central time instant of the selected time interval in a three-dimensional graph. The squared magnitude of the STFT yields the power spectrum. This so-called spectrogram is visualised in Fig. 6 for the 400–3500 Hz frequency range. To have a clear view negative frequency values were plotted. The main parameters for the STFT computation were:

SR: the sampling rate for the test;
N: the number of samples used to calculate the FFT, with $N = SR^{*}\Delta T$;
I: the time interval, over which the window moves to compute the next FFT, also called time precision.

The value (ΔT-I) is called the overlap. The time resolution ΔT and the frequency resolution Δf are calculated as follows:

$$\Delta T = N/SR$$

$$\Delta f = 1/\Delta T$$

It is always possible to increase N by adding zero values and thus get a better frequency resolution. For better view and analysis, the frequency projection (see Fig. 7) of the spectrogram was computed. The frequency projection is derived by projecting the spectrogram on the axis of frequency and power amplitude.

Not surprisingly, the maximum amplitude has a very high static value. This main lobe (which was not shown in Fig. 7 to be able to see the sidelobes) finished at 450 Hz. The following amplitude maximum corresponded to frequencies around 900 Hz, 1900 Hz, 2900 Hz; each lobe was about 1000 Hz wide.

So, the final specimen fracture could be detected clearly and can be characterised in time and frequency by this method which will also be used to study the damage initiation.

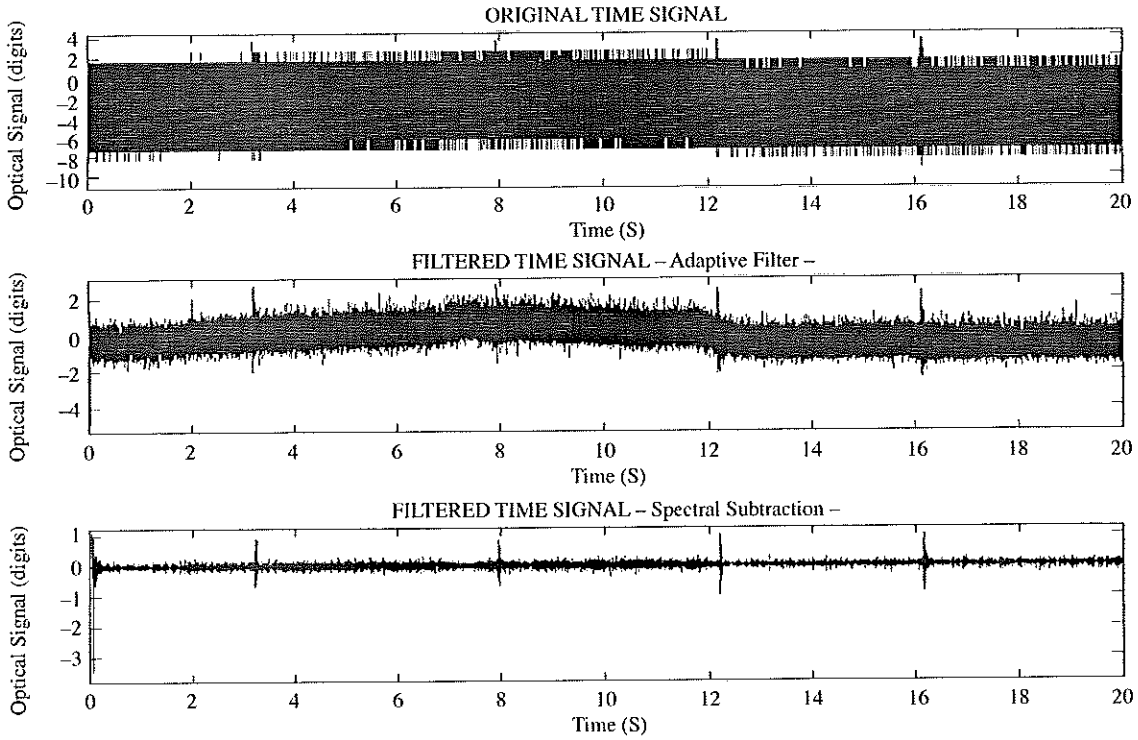


Fig. 9. The optical signal (time domain) during four successive pencil break tests on the surface of the specimen: the original signal (top) was sampled at 10 kHz, then it was filtered with an adaptive filter (middle) and the spectral subtraction method (bottom).

4.2. Damage initiation

4.2.1. Noise reduction:

One has to look for small effects on the optical signal. So, to increase the signal to noise ratio (SNR) several steps were taken.

A wide frequency range was first checked in order to detect transient phenomena. Tests were done with *SR* going from 10 to 250 kHz. First analysis showed that transient waves could be detected in the low frequency range (below 5 kHz). So the signals were downsampled to 10 kHz. The biggest noise source is from the laser

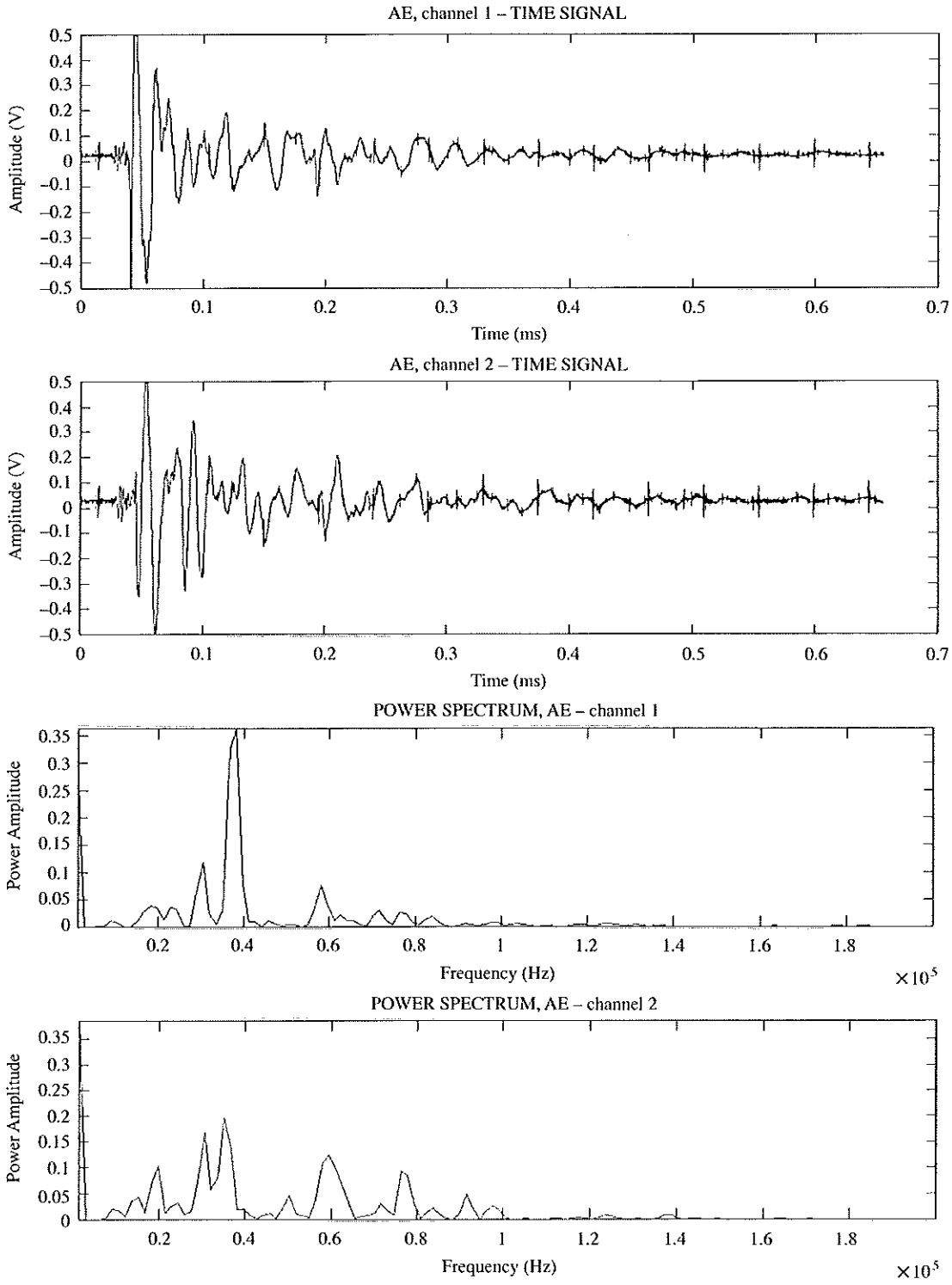


Fig. 10. AE signals for a typical in-plane pencil lead break test: time (top) and frequency (bottom) domains for both channels. The frequency range is from 1 to 200 kHz, $SR = 12.5$ MHz.

power supply (50 Hz and the harmonics from the net). An adaptive filter (LMS method, 2 taps) was used to remove this noise up to 1 kHz [27]. Using this filter was time consuming (computation time) therefore, since above 1 kHz this noise was small enough, the filtering was not applied above this frequency. Then, spectral subtraction, a filtering technique used in speech processing [28], was applied to see more clearly the expected 'optical events'. This technique requires that the background noise environment remains locally stationary to the degree that its expected spectral magnitude value just prior to an expected event equals its expected value during the event. It is also assumed that significant noise reduction is possible by removing the effect of noise from the magnitude spectrum only.

An example of these filtering techniques is shown in Fig. 8. The transient phenomena at the very beginning of the bottom curve are not revelant: the adaptive filter needs about 0.1 s to adapt, so in this time period the noise background is not stationary as it is required to use spectral subtraction. These curves show that 'something' (that will be called an 'optical event') is happening at

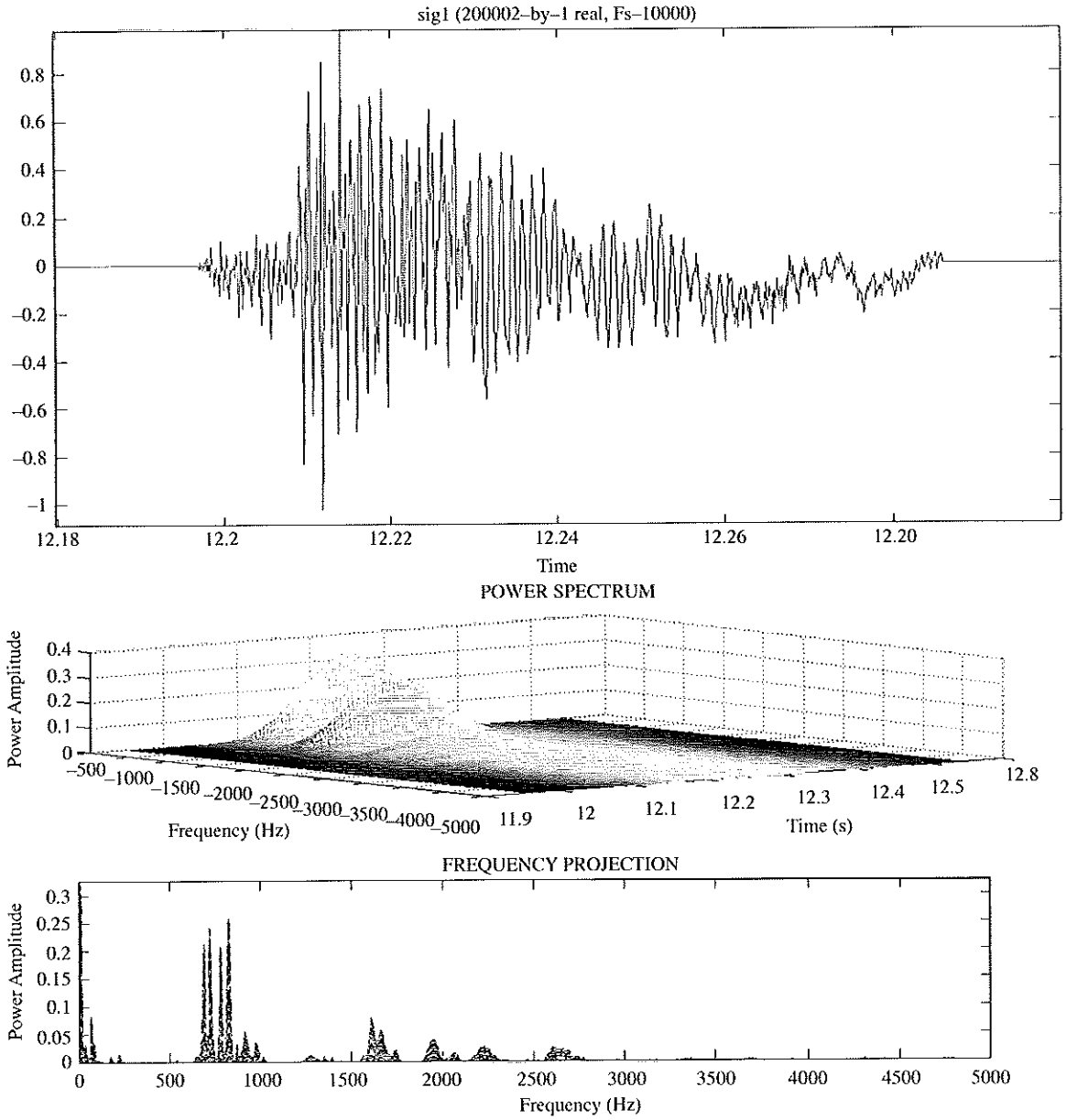


Fig. 11. The filtered optical signal for a pencil lead break test in the time domain (top). The STFT was computed ($\Delta f = 2.4$ Hz, $\Delta T = 410$ ms and $I = 5$ ms). Then, 3D plot (middle) and frequency projection (bottom) of the spectrogram were obtained.

time 0.25, 2.8 and 4.25 s. Next step is to link these with damage in the material. To do this, the AE data files have to be checked.

4.2.2. Pencil lead break tests:

Some pencil lead break tests were performed to calibrate the AE system. The optical system was also running during these tests (see Fig. 9).

The filtered optical signal corresponding to the third pencil lead break test in Fig. 9 (at time 12.2 s) was extracted and time-frequency analysis was performed as can be seen in Fig. 11. Both the AE time signal (seen in Fig. 10) and the optical time signal show clearly a small extensional component followed by a big flexural mode. This is coherent with what can be expected from a pencil lead break test done on the surface of the specimen.

The AE signal spectra show some wave packages in the low frequency range (below 140 kHz). According to M. Surgeon et al. [26], this is typical for a flexural mode. This is corroborated by checking the dispersive behaviour of this mode (the higher frequencies should propagate at higher velocities than the lower frequencies). The extensional mode is supposed to be found in the 400–800 kHz frequency range, but it is too small and is lost in the surrounding noise.

The optical signal (Fig. 11) shows some features similar with the AE signal. This is more apparent in the frequency domain. The wave packages in the low frequency range (below 3 kHz) are representative of a flexural mode. Unfortunately, the dispersive nature of this mode can not easily be detected for frequencies this low.

For pencil lead break tests on the surface of the specimen, it has been found that AE and optical results match well. These events can clearly be localised and characterised in the time domain and in the frequency domain. The flexural mode is identified. Tests on the edge of the specimen (for extensional mode detection) were also performed but no truly conclusive results could be produced so far.

4.2.3. Tensile tests, damage initiation

The optical and AE files have been checked independently. The AE system detects more events than the optical system, but a good correlation (in time) can be found with those detected by both systems. Nearly all

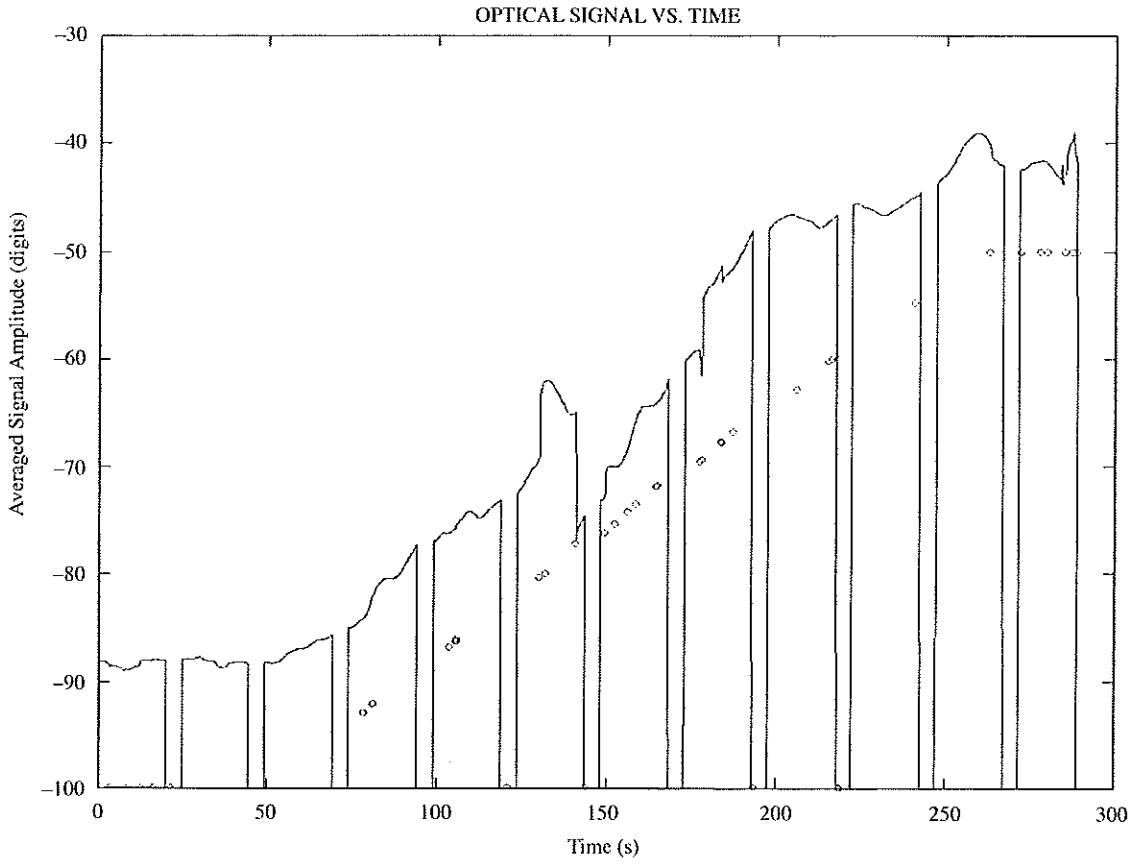


Fig. 12. The optical signal vs. time. The circles are the AE events vs. the load.

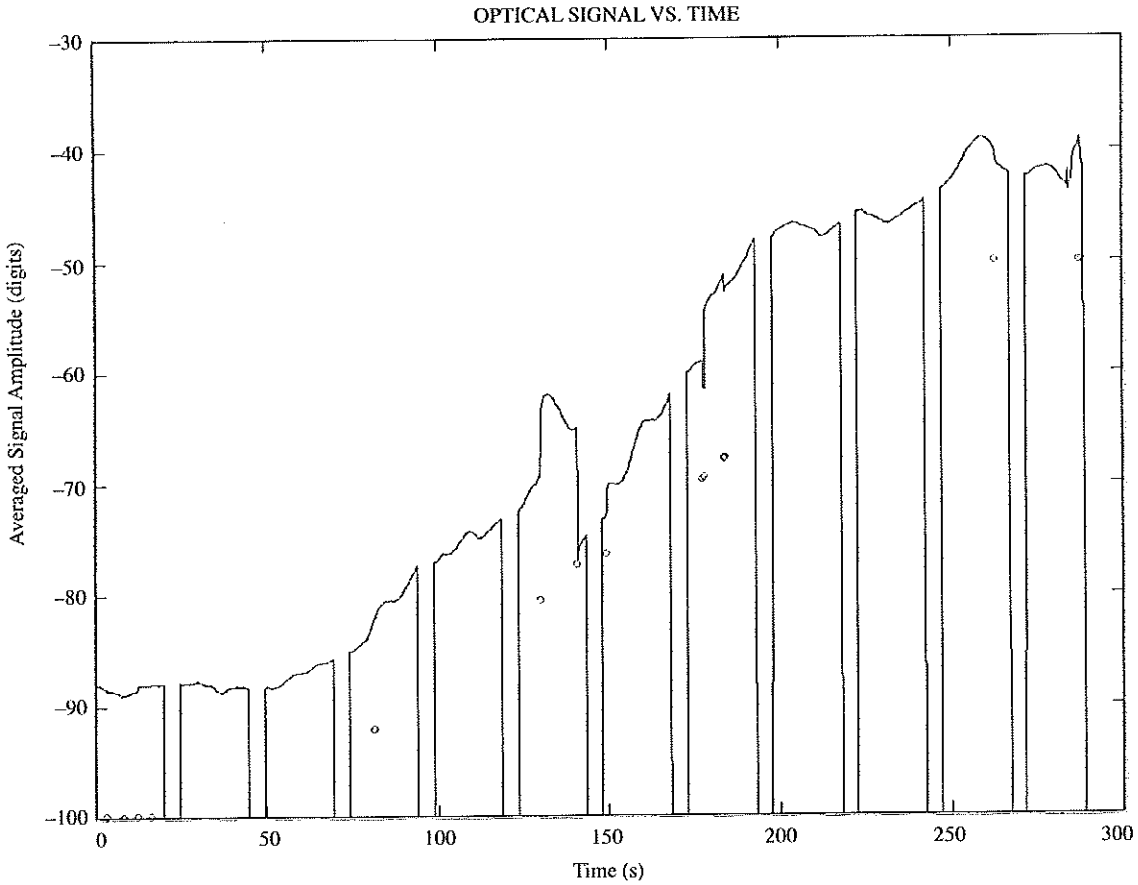


Fig. 13. The optical signal vs. time. The circles are AE events that could be linked to damage and were optically recorded. The four first ones are pencil lead break tests used for calibration.

the events detected optically can be found in the AE files. This may imply a higher sensitivity for the AE system. But this sensitivity is directly linked to the amplifier setting and often events detected by AE are in fact noise (EMI, grip noise).

The AE events were sorted from the AE data files according to several criteria, namely their amplitude, duration, energy and number of ringdown counts. Only the most energetic events were also detected by the optical system. All the events whose energy was above 10^5 eV were detected, no event whose energy was less than 2.5 10^4 eV could be optically sensed. No data events were available between these two values.

Studies are under way to determine the exact sensor sensitivity and bandwidth. So far, the main emphasis has been put on increasing the SNR via filtering techniques. Fig. 12 shows a time-averaged optical signal versus time. Only the adaptive filter was applied to the signal, and then it was averaged (one point on the curve corresponds to the signal mean value over a 0.1 s interval). The circles also plotted on this graph are the AE events (MAE system); the vertical scale is proportional to the load curve. The five first ones correspond to pencil lead break tests used for the calibration. The load curve is clearly linear (the vertical values for the last ones are not revelant because of saturation).

The loading began after 50 s of test, the slope of the optical signal changes at the same time. Near the end of the test (before the final specimen failure) the slope is also decreasing, this may be a first indication that the optical signal contains information about the applied load.

Fig. 13 is the same curve but only the AE events that could be clearly related to damage are plotted [26]. It can be seen that they all correspond to an important irregularity in the optical curve. An explanation for this result is that the optical signal contains information about the strains inside the material. These strains are due to the loading (remote forces) but are also due to the damage initiated in the material.

Most of the events are localised between 130 and 180 s. At the beginning of this period, there is an important increase in the optical signal. It happens again, but to a lesser extent, before the final fracture (at time 260 s). This kind of phenomenum seems to be quite common and may be an early indicator for damage. Further studies are needed to find a satisfactory explanation for this.

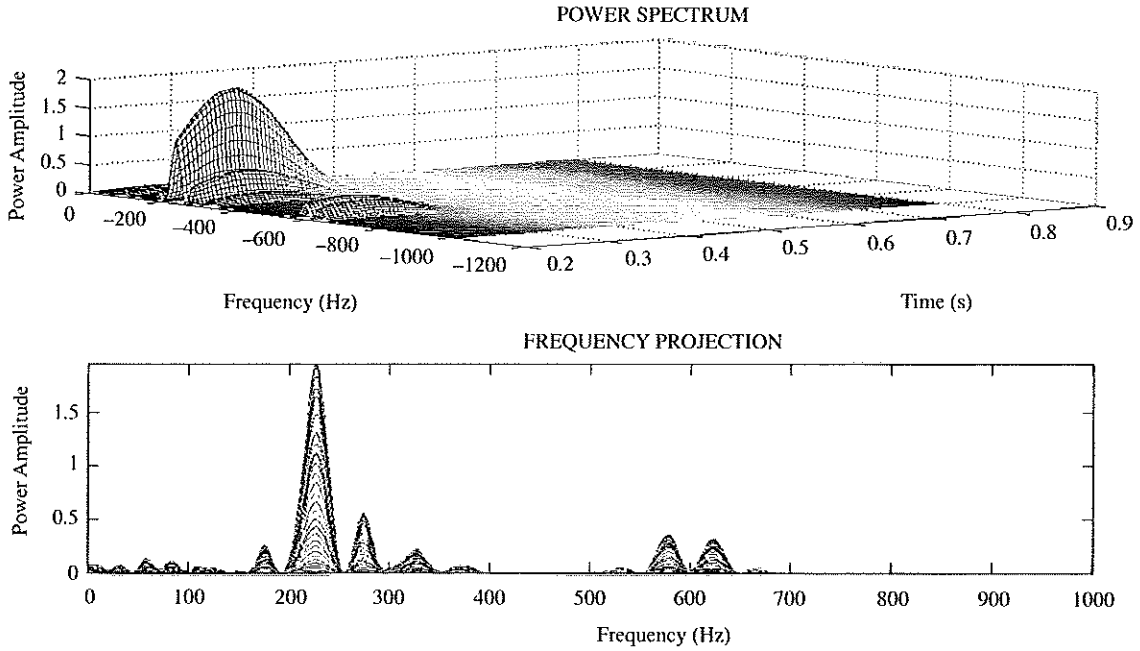


Fig. 14. 3D plot and frequency projection of the spectrogram ($\Delta f = 2.4$ Hz, $\Delta T = 410$ ms, $I = 5$ ms) of the optical event seen at time 0.25 s in Fig. 8. Classical AE says it corresponds to fibre fracture.

Fig. 14 is an example of an optical event that is related to damage inside the material. Classical AE parameters corresponding to this optical event are:

Amplitude:	93.9 dB (saturation)
Duration:	2.4 ms
Energy:	1.9 10^6 eV
Ringdown Counts:	578

According to the high amplitude value, this event corresponds to fibre bundle fracture [22]. This is corroborated by the fact that the event occurs very late in the tensile test. So real damage can be detected with the optical sensor. It can be characterised in the frequency domain, which should allow damage identification.

Time-frequency analysis allows to detect phenomena that cannot be seen in the time domain. Analysis of the signal frequency content seems to indicate the presence of frequencies characteristic to damage initiation. It should also permit the circumvention, at least partially, of the problem of intensity fluctuations not related with strain (ambient vibration for instance).

5. Conclusion

It has been shown that an intensity modulated optical sensor based on the microbending concept can be used for continuous damage monitoring. It is simple and robust but requires some advanced signal analysis tools like adaptive filtering, spectral subtraction filtering, and time-frequency analysis (STFT).

The principle has been proven to work. The sensor can detect damage initiation and characterise its frequency content. The similarities between optical and MAE signals should permit damage identification. To achieve this, the next steps are:

- to use only MAE (Wave Explorer System) for AE. Other techniques, like edge replica, may also be useful for better damage characterisation;
- to optimise the experimental setting to increase the SNR, to lower the time resolution, and to apply the load continuously;
- to use other signal analysis tools, for instance the STFT is not the best tool to study low frequency transient phenomena. The Wavelet Toolbox might offer an alternative.

The damage location has not been studied so far, this may require embedding several optical fibres in the specimen.

Acknowledgements

The authors would like to thank Ing. J. Vanhulst for his invaluable help with the data acquisition system and K. Eneman for providing the code for the applied filtering techniques. S. Van Huffel and M. Wevers are senior research associates of the F.W.O. (Fund for Scientific Research — Flanders).This work was supported by the F.W.O. Project no. G.0200.00, by the Belgian Programme on Interuniversity Poles of Attraction

(IUAP-4/2 & 24), initiated by the Belgian State, Prime Minister's Office for Science, and by a Concerted Research Action (GOA) project of the Flemish Community, entitled "Mathematical Engineering for Information and Communication Systems technology".

References

[1] Culshaw B, Dakin J. Optical fibre sensors: systems and applications 1989;II:727–45.
[2] Krohn DA. Fibre optic sensors: fundamental and applications. Instrument Society of America, 1988 (pp. 1–61).
[3] Gandhi MV, Thompson BS. Smart materials and structures. 1992 (pp. 217–288).
[4] Measures RM. Advances toward fiber optic based smart structures. Optical Engineering 1992;31(1):34–47.
[5] Kwon IB, Kim CG, Hong CS. Simultaneous sensing of the strain and points of failure in composite beams with an embedded fiber optic Michelson sensor. Composite Science and Technology 1997;57:1639–51.
[6] Bhatia V, Schmid CA, Murphy KA, Claus RO, Tran TA, Greene JA, Miller MA. Optical fiber sensing technique for edge-induced and internal delamination detection in composites. Smart Mater Struct 1995;4:164–9.
[7] Tran TA, Miller III WV, Murphy KA., Vengsarkar AM, Claus RO. Stabilized extrinsic fiber optic Fabry-Perot sensor for surface acoustic wave detection. Proceeding of SPIE, vol. 1584, Fiber Optic and Laser Sensors 1991; IX; p. 178–86.
[8] Claus RO, Gunther MF, Wang A, Murphy KA. Extrinsic Fabry-Perot sensor for strain and crack opening displacement measurements from −200 to 900°C. Smart Mater Struct 1992;1:237–42.
[9] Tsuda H, Ikeguchi T, Takahashi J, Kemmochi K. Damage monitoring of carbon-fiber-reinforced plastics using Michelson interferometric fiber-optic sensors. Journal of Materials Science Letters 1998;17:503–6.
[10] Berthold JW. Historical review of microbend fiber-optic sensors. J Lightwave Technology 1995;13(7):1193–9.
[11] Glossop NDW, Dubois S, Tsaw W, Leblanc M, Lymer J, Measures RM, Tennyson RC. Optical fibre damage detection for an aircraft composite leading edge. Composites 1990;21(1).
[12] Waite SR, Sage GN. The failure of optical fibres embedded in composite materials. Composites 1988; 19(4).
[13] Lawson CM, Tekippe VJ. Environmentally insensitive diaphragm reflectance pressure transducer. Proceeding of SPIE 1983;412:96–103.
[14] Berthold JW, Ghering WL, Varshneya D. Design and characterization of a high temperature fiber-optic pressure transducer. J Lightwave Technology 1987;5:870–6.
[15] Yao SK, Asawa CK. Microbending fiber optic sensing. Proceeding of SPIE 1983;412:9–13.
[16] Surgeon M. Continuous damage monitoring techniques for laminated CFRP composite material. PhD thesis, KU Leuven, 1999.
[17] Eaton NC, Curran MJ, Dakin JP, Geiger H. Factors affecting the embedding of optical fibre sensors in advanced composite structures. AGARD Conference Proceedings 531, 75th Meeting, 5–7 October 1992, p. 20.1–20.14.
[18] Roberts SSJ, Davidson R, Paa R. Mechanical properties of composite materials containing embedded fibre-optic sensors. Fibre optics smart structures and skin IV; Proceedings of the meeting, Boston, MA, 5–6 September 1991, Bellingham, WA, SPIE vol. 1588, p. 326–341.
[19] Jensen DW, Pascual J, August JA. Performance of raphite/bismaleimide laminates with embedded optical fibres. Part I: uniaxial tension. Part II: uniaxial compression. Smart Material Structure 1992;1:24–30, 31.
[20] Coenen L. The influence of embedding optical fibres on the mechanical properties of a carbon fibre composite and monitoring the damage development using the acoustic emission technique. Master thesis, KU Leuven,1995.
[21] Surgeon M, Wevers M. Static and dynamic testing of a quasi isotropic composite with embedded optical fibres. Composites Part A 1999;30(4):317–24.
[22] van Huffel S, Craemers J, Lenaerts B, Daniels H, Naulaers G, Casaer P. Episodes of apnea and bradycardia in the preterm newborn: impact on cerebral oxygenation measured by near infrared spectrophotometry. Proceeding of EUROPTO Conference on Photon Propagation in Tissues IV, Sweden, 1998, SPIE vol. 3566, p. 112–23.
[23] Wevers M. Listening to the sound of materials: acoustic emission for the analysis of material behaviour. NDT&E International 1997;30(2):99–106.
[24] Ziola S, Searle I. Automated source identification using modal acoustic emission. Review of Progress in Quantitative Nondestructive Evaluation 1997;16A:413–9.
[25] Gorman MR. Progress in detecting transverse matrix cracking using modal acoustic emission. Review of Progress in Quantitative Non-destructive Evaluation 1998;17A:557–64.
[26] Surgeon M, Wevers M. Continuous damage monitoring techniques for laminated composite materials. Proceeding of ICCM-12 Europe Conference, 5–9 July 1999, Paris.
[27] Proakis JG, Manolakis DG. Digital signal processing: principles, algorithms, and applications. 3rd ed. Upper Saddle River, NJ: Prentice Hall, 1996.
[28] Boll SF. Suppression of acoustic noise in speech using spectral subtraction. IEEE Transactions on Acoustics, Speech, and Signal Processing 1979; ASSP-27(2).